



Australian Government
Department of Defence
Defence Science and
Technology Organisation

Restrictions on the Ratio of Normal to Tangential Field Components in Magnetic Rubber Testing

S. K. Burke and M. E. Ibrahim

Maritime Platforms Division
Defence Science and Technology Organisation

DSTO-TR-1991

ABSTRACT

Magnetic Rubber Testing (MRT) is an extremely sensitive method for detecting surface-breaking cracks in ferromagnetic materials, and is used extensively in critical inspections for D6ac steel components of the F-111 aircraft. This report documents a series of experiments, performed to investigate the effect of normal versus tangential magnetic field components in MRT. The results confirm that excessive levels of normal (perpendicular) magnetic field in active-field MRT procedures can cause distortion, weakening or masking of indications from fatigue cracks. Consequently, recommendations are made for the restriction of normal field levels in the development of active-field MRT procedures. This work does not deal with residual-field MRT, and the recommendations supplied herein are not transferable to residual-field measurements.

RELEASE LIMITATION

Approved for public release

Published by

*Maritime Platforms Division
DSTO Defence Science and Technology Organisation
506 Lorimer St
Fishermans Bend, Victoria 3207 Australia*

*Telephone: (03) 9626 7000
Fax: (03) 9626 7999*

© Commonwealth of Australia 2007

*AR-013-900
July 2007*

APPROVED FOR PUBLIC RELEASE

Restrictions on the Ratio of Normal to Tangential Field Components in Magnetic Rubber Testing

Executive Summary

Magnetic Rubber Testing (MRT) is an extremely sensitive method for detecting surface-breaking cracks in ferromagnetic materials. It is used extensively in critical inspections for the D6ac steel components of the F-111 aircraft. As a result of uncertainties in the understanding of MRT raised by the RAAF Non-Destructive Testing Standards Laboratory (NDTSL), DSTO was requested to investigate the role of the normal versus tangential components of magnetic field in MRT and its effect on crack detection.

The results of a series of experiments to investigate the effect of normal versus tangential field components in MRT are presented in this report. The results confirm that excessive levels of normal (perpendicular) magnetic field in active-field MRT procedures can cause distortion, weakening or masking of indications from fatigue cracks. Consequently, when developing active-field MRT procedures, the levels of normal magnetic fields should be reduced as much as practicable. The experimental results show that, provided that throughout the test area the normal component of the magnetic field does not exceed the tangential magnetic field, the presence of a normal magnetic field should not significantly reduce the sensitivity of active-field MRT.

The experimental results also demonstrated that, for active-field MRT, a tangential field in the range 25–30 Gauss is suitable to provide clear MRT indications for the laboratory-grown fatigue cracks in the test coupons used.

Consequently, it is reasonable to conclude that an active-field MRT inspection developed to achieve 25–30 Gauss tangential magnetic field throughout the test area, and with the normal field not exceeding the tangential magnetic field throughout the test area, should achieve the levels of sensitivity and reliability normally expected for active-field MRT.

The scope of this work did not include residual-field MRT and results should not be applied to any residual-field MRT procedures.

Authors



Dr Stephen K. Burke
Maritime Platforms Division

Dr Burke was awarded a B.Sc. (Hons) from Monash University and a Ph.D. from Imperial College London in 1980. He is a Fellow of the Australian Institute of Physics (FAIP) and a Chartered Physicist (C. Phys). Dr Burke is Head of the NDE R&D Group at DSTO Melbourne.



Mr Matthew E. Ibrahim
Maritime Platforms Division

Matthew holds a B.Sc. in physics, and an M.Sc. in theoretical and experimental NDE from Monash University. He is a member of the Australian Institute of Physics (MAIP), and has performed NDE research for the Defence Science and Technology Organisation since 1998.

Contents

ABBREVIATIONS AND SYMBOLS

| | |
|---|-----------|
| 1. INTRODUCTION | 1 |
| 2. NORMAL AND TANGENTIAL FIELDS | 1 |
| 2.1 Initial DSTO Experiments..... | 2 |
| 2.2 Experiments with uniform applied normal fields..... | 4 |
| 2.2.1 Interim normal field restriction | 5 |
| 2.3 An improved Normal-to-Tangential Field Ratio for MRT | 6 |
| 2.3.1 Mousehole Coupon Experiment: Design. | 6 |
| 2.3.2 Mousehole Coupon Experiment: Results..... | 7 |
| 2.3.3 Mousehole Coupon Experiment: Analysis | 11 |
| 3. DISCUSSION..... | 11 |
| 4. CONCLUSIONS | 12 |
| 5. RECOMMENDATIONS | 13 |
| 6. ACKNOWLEDGEMENTS..... | 13 |
| 7. REFERENCES..... | 13 |
| APPENDIX A: NORMAL-TANGENT FIELD TRIAL RESULTS..... | 15 |
| APPENDIX B: INSPECTION PROCEDURE | 17 |
| APPENDIX C: STATISTICAL ANALYSIS OF THE LENGTHS OF MRT | |
| INDICATIONS FOR THE CASES M1, M2 AND M3 | 23 |
| C 1 Experimental scatter | 23 |
| C 2 Tests of statistical significance | 23 |

Abbreviations and Symbols

| | |
|--------------------|---|
| a_{NDI} | The assumed size of the largest defect that will be missed in an inspection |
| AC | Alternating Current |
| Active field MRT | Magnetic field applied during rubber cure |
| B | Magnetic induction |
| B_n | Magnetic induction normal (perpendicular) to the surface being tested |
| B_t | Magnetic induction tangent (parallel) to the surface being tested |
| DC | Direct Current |
| DSTO | Defence Science and Technology Organisation |
| FFVH | Fuel Flow Vent Hole |
| Mousehole | Fuel Flow Vent Hole |
| MPI | Magnetic Particle Inspection |
| MRT | Magnetic Rubber Testing |
| NdFeB | Neodymium Iron Boron |
| NDT | Non-Destructive Testing |
| NDTSL | Non-Destructive Testing Standards Laboratory |
| POD | Probability Of Detection |
| Residual Field MRT | Magnetic field removed before rubber is poured |

1. Introduction

Magnetic Rubber Testing (MRT) is a sensitive method for detecting surface-breaking cracks in ferromagnetic materials. It is used extensively in critical inspections of the D6ac steel components in the F-111 aircraft. As a result of uncertainties in the understanding of MRT raised by the RAAF Non-Destructive Testing Standards Laboratory (NDSTL), DSTO was requested to investigate the following issues:

- The differences between the residual and active field methods of MRT, especially with respect to the differences for shallow defects;
- The basis for verification of adequate residual field strength in the region of interest;
- The cause of apparent reduction in measured length compared to true crack length;
- The effect of normal versus tangential fields and the significance on defect detection; and
- The feasibility of using modelling techniques to evaluate field strength for critical inspection regions.

In this document, we present the results of a careful study on the effect of normal versus tangential fields in MRT and provide recommendations for the maximum permissible values for the normal component of the magnetic field in active-field MRT.

2. Normal and Tangential Fields

In current active-field MRT practice, the magnetic field should be tangent (parallel) to the surface of the part to be inspected throughout the test area, which encompasses the possible crack locations. It has been generally assumed that if the measured tangential field is within prescribed limits (typically 25 – 30 Gauss¹), the magnetisation will be adequate to ensure the required MRT sensitivity.

A critical inspection area in the F-111 wing structure is the Fuel Flow Vent Hole (FFVH) or “mousehole” [Watters, 1997]. Previous Probability of Detection (POD) trials performed using active-field MRT on a mousehole-geometry support the proposal that a tangential field of 25 Gauss measured at the test area is sufficient to achieve an $a_{\text{NDI}} < 0.020$ inches^{2,3}, provided the component has a good surface finish [Harding and Hugo, 2002]. However, subsequent laboratory trials at NDTSL have suggested that the presence of a significant magnetic field normal (perpendicular) to the surface may adversely affect the clarity and length of MRT indications. Since for the previous active-field MRT POD trial the normal field was nominally zero, there is a need to investigate the influence of normal magnetic fields on MRT sensitivity and reliability.

¹ CGS (EMU) units are used in this report for magnetic flux density: 1 Gauss = 0.1 mT

² Imperial units are used in this report for crack dimensions: 1” = 25.4 mm

³ a_{NDI} is the minimum crack length which can be reliably detected by the NDT procedure

2.1 Initial DSTO Experiments

Initially, experiments were performed with various methods of continuous (active-field) magnetisation to generate different ratios of the normal to tangential field in a single test specimen. The component inspected contained two boltholes, typical of those found on an F-111, with artificially grown corner and bore fatigue cracks (Figure 1). The magnetic field components both tangent and normal to the location on the surface to be inspected were measured using a Hall-effect probe. The hole inspected (hole A in coupon BH-27) contained a corner crack with a surface length of 0.027" on the surface and 0.033" in the bore. ⁴

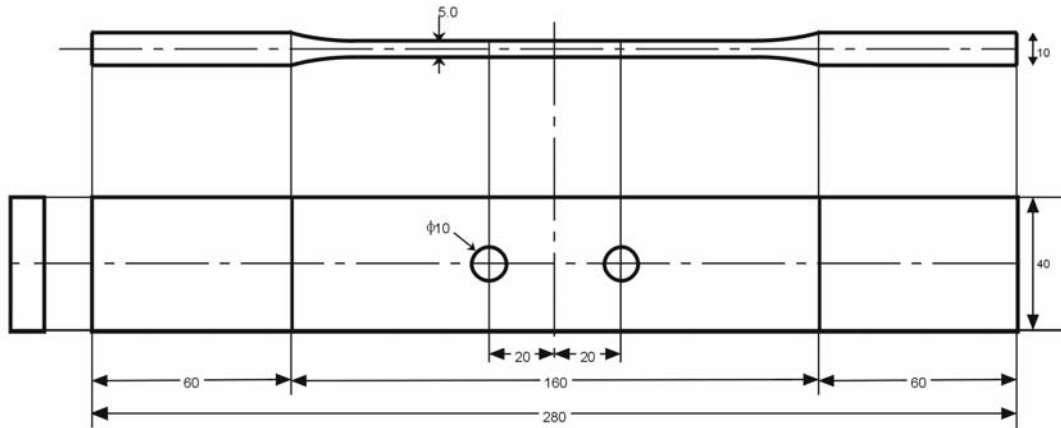


Figure 1. Bolthole coupon, made of D6ac steel and featuring two boltholes of typical F-111 dimensions. The boltholes had fatigue cracks grown in them using representative F-111 flight spectrum loading.

Three different magnetisation configurations were used on the coupon in order to vary the ratio of the fields measured tangent (B_t) and normal (B_n) to the surface:

- In the first case, a power-shoe closed-circuit magnet with pole pieces was used (Figure 2a). Here $B_n \sim 5$ Gauss and $B_t \sim 20$ Gauss so that the normal component of field was small and the ratio of normal-to-tangential field components B_n/B_t was ~ 0.2 . The resulting cast shows a clear indication with particle draw-out on both sides of the crack (as shown by the surface crack micrograph in Figure 2b).
- In the second case, two NdFeB (Neodymium-Iron-Boron) bar magnets were used to force the magnetic flux through the specimen and out the opposite side (Figure 3a). This configuration produced a very large normal field ($B_n \sim 50$ Gauss with $B_t \sim 16$ Gauss) and the ratio B_n/B_t was ~ 3 . The crack indication remained strong and was very slightly reduced in length (Figure 3b). The broad white band immediately to the right of the indication is an indicator of a large normal field component and arises from enhanced particle draw-out on one side of the crack.
- The third configuration employed the same two NdFeB bar magnets as the previous case but arranged to create an open magnetic circuit as shown in Figure 4a.

⁴ Crack dimensions were determined by DSTO in POD trial master inspections, using active field MRT with specimens under an applied tensile load in order to open the cracks (Harding and Hugo, 2002).

Here $B_n \sim 80$ Gauss and $B_t \sim 20$ Gauss so that the normal component of field was even larger than previously and the ratio of B_n/B_t was ~ 4 . The resulting MRT cast (Figure 4b) showed particle draw out on one side only, a significant reduction in crack length, and a change-over of the white band near the tip of the crack from left to right.

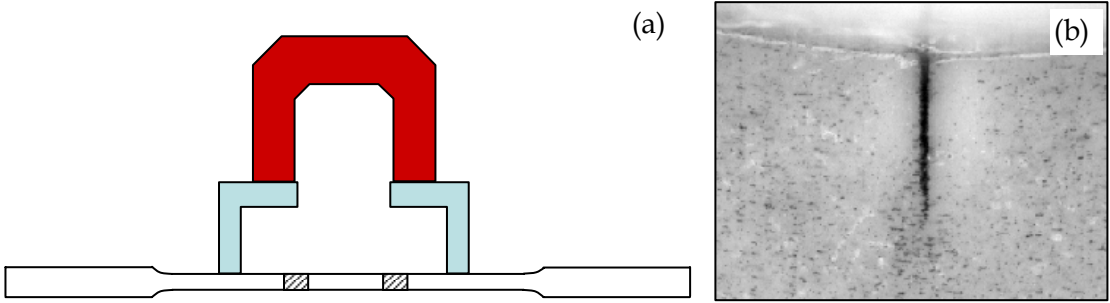


Figure 2. (a) Active field MRT cast performed with a power-shoe magnet and steel pole pieces forming a closed magnetic loop, and (b) resulting cast on the surface. Here $B_n \sim 5$ Gauss, $B_t \sim 20$ Gauss and $B_n/B_t \sim 0.2$.

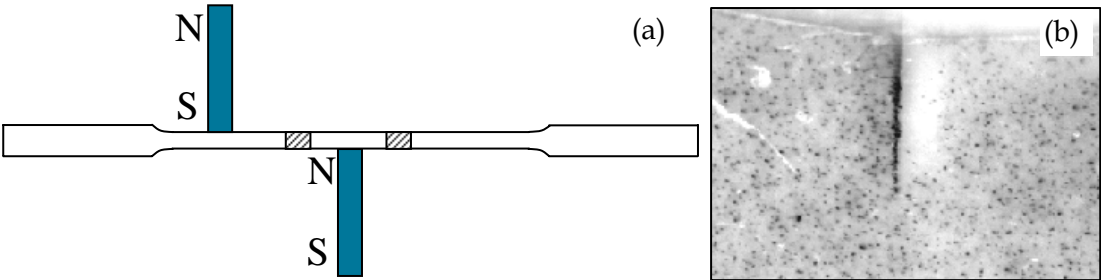


Figure 3. (a) Active field MRT cast performed with two bar magnets forming a magnetic flux path across the diameter of the bolthole, and (b) the resulting cast on the surface. Here $B_n \sim 50$ Gauss, $B_t \sim 16$ Gauss and $B_n/B_t \sim 3$.

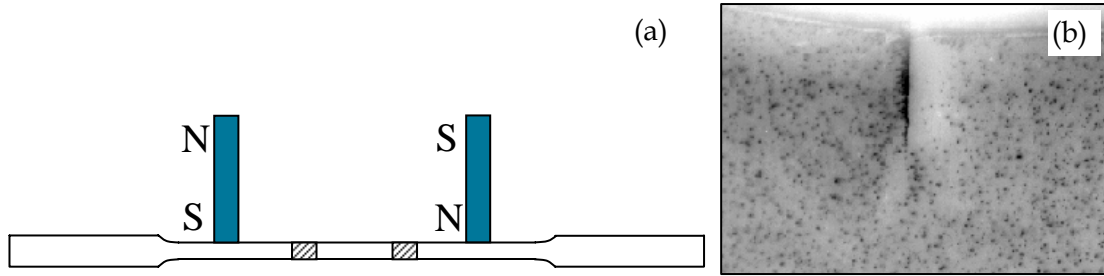


Figure 4. (a) Active field MRT cast performed with two bar magnets forming an open circuit, and (b) the resulting cast on the surface. Here $B_n \sim 80$ Gauss, $B_t \sim 20$ Gauss and $B_n/B_t \sim 4$. (The micrographs of the surface crack in Fig.2b, 3b and 4b have the same magnification)

These preliminary experiments demonstrated that a large normal component of field could lead to a significant reduction in crack-indication length and white-banding (ghosting), with possible adverse effects on crack detectability.

As these preliminary configurations did not allow accurate measurement and control of the field components, further experiments were performed in which the normal component of magnetic field could be more carefully controlled through the use of a Helmholtz coil. The results are described in the following Section.

2.2 Experiments with Uniform Applied Normal Fields

A second series of experiments was performed with the same bolthole specimen using a pair of Helmholtz coils, as shown in Figure 5. The Helmholtz coils consist of a pair of identical coaxial coils separated by one coil radius. When energised, these coils generated a uniform field at their centre which extends over the cracked region of interest in the bolthole specimen. Variation of the coil current allowed for more precise control of the normal field component at the coupon while keeping the tangential component constant.

In this series of experiments, the coil current was supplied by a DC power supply and the normal field could be varied up to a maximum field of 17 Gauss with the tangent field held constant at 26 Gauss using permanent magnets. Typical casts, shown in Figure 6a and Figure 6b, show strong and clear crack indications with the correct length. These results demonstrate that, provided the tangential field is within valid limits, the performance of continuous field MRT should not be degraded provided the ratio of the normal field to tangent field B_n/B_t is less than ~ 0.65 .

The degradation in MRT performance with increasing normal component of field is illustrated by the cast shown in Figure 6c for which the normal field was provided by an arrangement of permanent magnets rather than the Helmholtz coil and the ratio $B_n/B_t = 3.3$. Here, the length of the indication is reduced and the single-sided white banding effect of particle draw-out on only one side of the crack is evident.

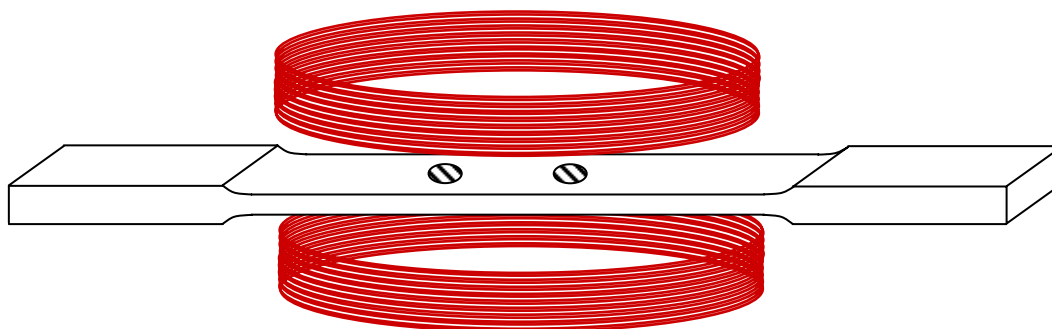


Figure 5. Helmholtz coils surrounding the bolt-hole coupon BH-27 (schematic). These coils generate a uniform incident normal field in the vicinity of the crack. NdFeB magnets (not shown) placed at either end of the specimen provide the tangential field of 26 Gauss.

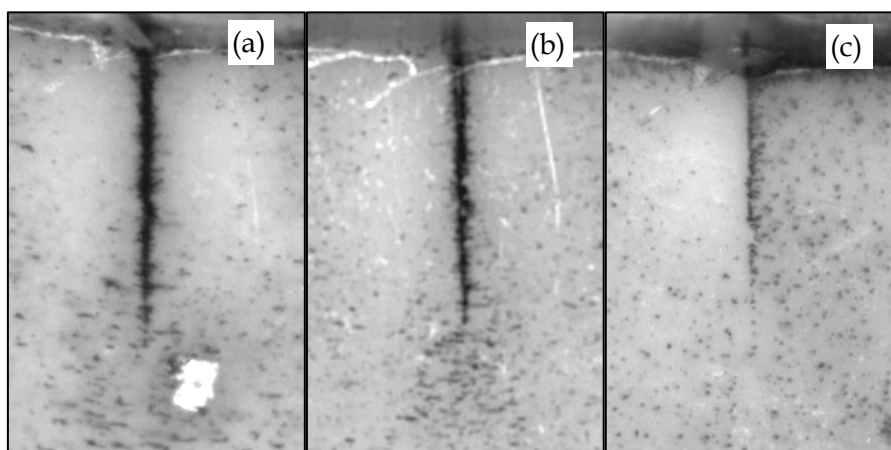


Figure 6. Surface crack indications for active field measurements on bolt-hole coupon BH-27. (a) MRT cast for $B_t = 26$ Gauss, $B_n = 0$ Gauss and $B_n/B_t = 0$; (b) MRT cast for $B_t = 26$ Gauss, $B_n = 17$ Gauss and $B_n/B_t = 0.65$. Also shown, Cast (c), where a permanent magnet was used to augment the normal field, $B_t = 20$ Gauss, $B_n = 67$ Gauss and $B_n/B_t = 3.3$. (Identical magnification in all cases)

2.2.1 Interim Normal Field Restriction

The results of the experiments to this point were summarised by an interim requirement that the normal field should be kept as small as possible and, in the worst case, that “the tangent field should be at least twice the normal component”. This advice was communicated to NDTSL and subsequently adopted.

This interim requirement imposed a considerable burden on MRT procedure development as it became increasingly evident that the requirement was difficult to satisfy in practice for many geometries and greatly added to the complexity of the MRT procedures. As a result of this feedback, a final series of measurements was performed to establish a valid, but more workable, upper limit for the normal field.

2.3 An Improved Normal-to-Tangential Field Ratio for MRT

The final series of experiments⁵ was designed to establish whether the interim recommendation that “the tangent field should be at least twice the normal component” could be extended to allow a ratio where “the tangent field should be greater than or equal to the normal component”.

2.3.1 Mousehole Coupon Experiment: Design.

The experiments were performed using six of the D6ac “mousehole” test specimens containing fatigue cracks which had been prepared by DSTO for an earlier POD study carried out jointly with NDTSL [Harding and Hugo, 2002]. The specimens contained a total of 19 confirmed fatigue cracks in the region of interest, with a total of 2 confirmed corner cracks and 17 confirmed bore cracks.

The estimated crack lengths in the specimens (the so-called ‘master’ crack lengths) are given in Appendix A and were taken from the results of the MRT master inspections performed under tensile load as part of the earlier POD study. These master crack lengths were shown to be a good estimate of the true crack length obtained from fractography [Harding and Hugo, 2002]. Most of the cracks were in the length range 0.005” to 0.010”. The largest crack was a 0.090” corner crack. There were also numerous cracks < 0.005” for which the crack lengths had not been formally recorded in the POD trial.

MRT casts were obtained for each of the mousehole coupons under three magnetic field conditions by rotating a power-shoe permanent magnet about the axis of the hole. The field conditions were:

- Magnet position 1 (M1). Tangent field between 25 - 30 Gauss, normal field less than 6 Gauss
- Magnet position 2 (M2). Tangent field between 25 - 30 Gauss, normal field equal to the tangent field
- Magnet position 3 (M3). As for M2 but with the normal field reversed (ie tangent field between 25 - 30 Gauss, normal field equal to the tangent field but opposite in sign).

The length of the crack indications in the bore was measured off the casts using an optical microscope. The test procedure is reproduced in Appendix B and the three magnet positions are shown schematically in Figures P5 - P7 of Appendix B.

Accurate and repeatable measurements of the normal and tangential magnetic field components in the test region were assisted by using a precisely machined Gaussmeter probe guide which could be inserted into the hole during magnet set up. From the symmetry of the experiments, a change in the sign of the normal component of the magnetic field should not change the length of any crack indication. This symmetry condition acts as a check on the size of the experimental uncertainties.

⁵ This trial was performed by AerostructuresNDT, Melbourne under contract to DSTO.

2.3.2 Mousehole Coupon Experiment: Results

The measured crack indication lengths for the three magnetisation conditions and six test specimens are presented in the form of histograms in Figure 7 to Figure 12. The results are also summarised in numerical form in Appendix A.

One of the characteristic features of the MRT indications for the mousehole experiments is also shown in Figure 13 where the crack indication is bordered by distinct white bands (magnetic-particle-free regions). The white banding is symmetrical about the crack for small normal fields (M1), lies on one side of the crack when the normal field is larger (M2) and reverses sides when the normal field is reversed (M3). In fact, the location of the single white band in (b) and (c) is a clear indication of the presence of a significant normal field. This behaviour is consistent with simple theories for the motion of ferromagnetic particles in the vicinity of a crack (see section 3).

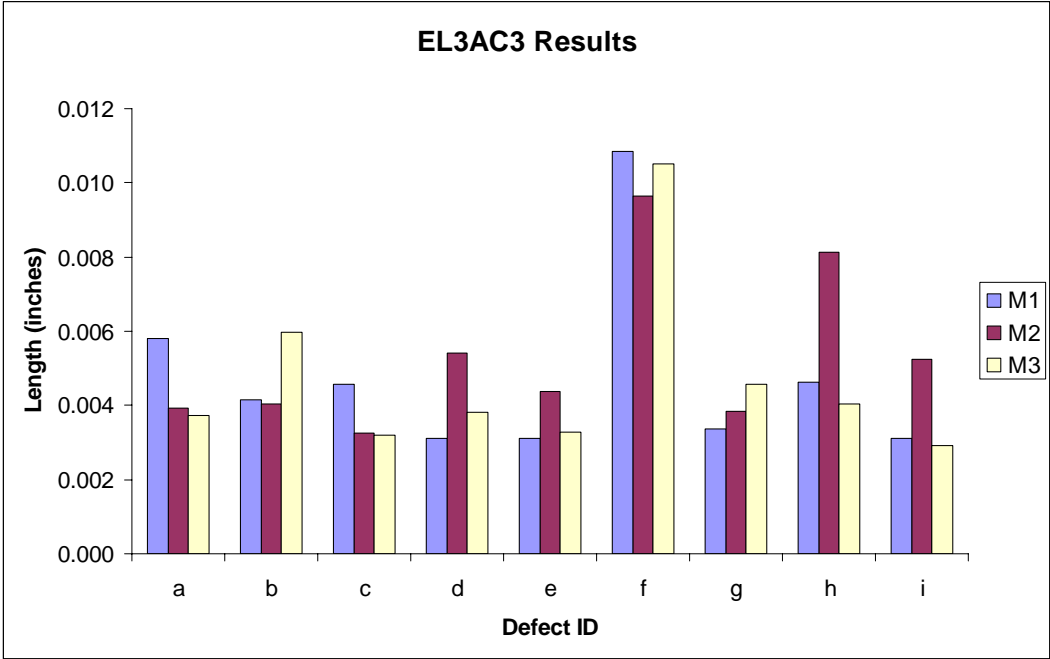


Figure 7. Measured defect indication lengths for fatigue cracks in the D6ac mousehole specimen EL3AC3 for field configurations M1, M2 and M3 (Appendix A). There is no significant difference in the length of the crack indications for the different field configurations.

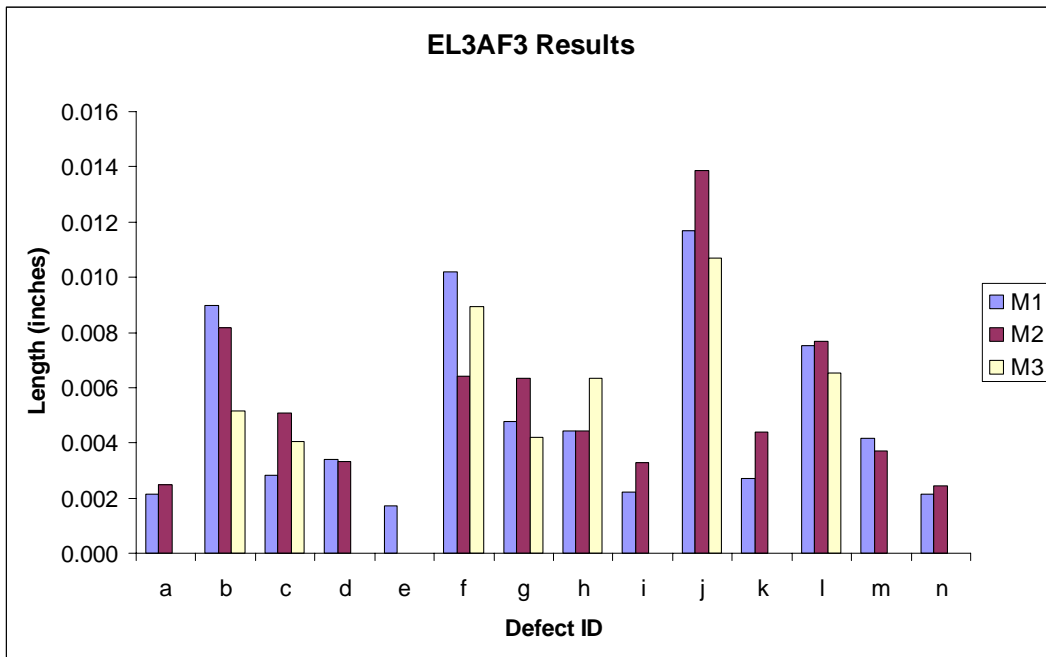


Figure 8. Measured defect indication lengths for fatigue cracks in the D6ac mousehole specimen EL3AF3 for field configurations M1, M2 and M3 (Appendix A). There is no significant difference in the length of the crack indications for the different field configurations.

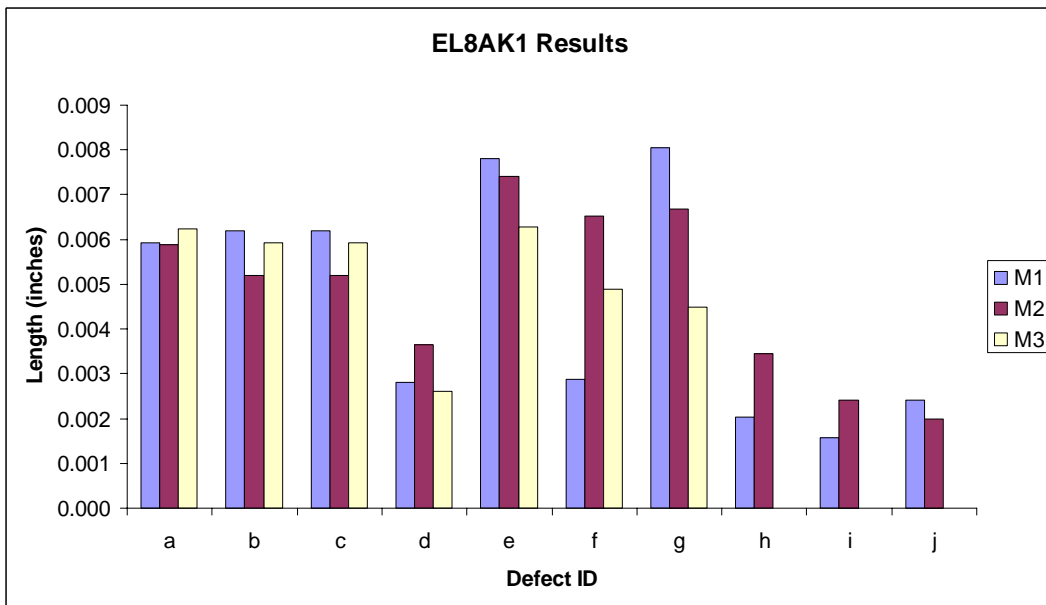


Figure 9. Measured defect indication lengths for fatigue cracks in the D6ac mousehole specimen EL8AK1 for field configurations M1, M2 and M3 (Appendix A). There is no significant difference in the length of the crack indications for the different field configurations.

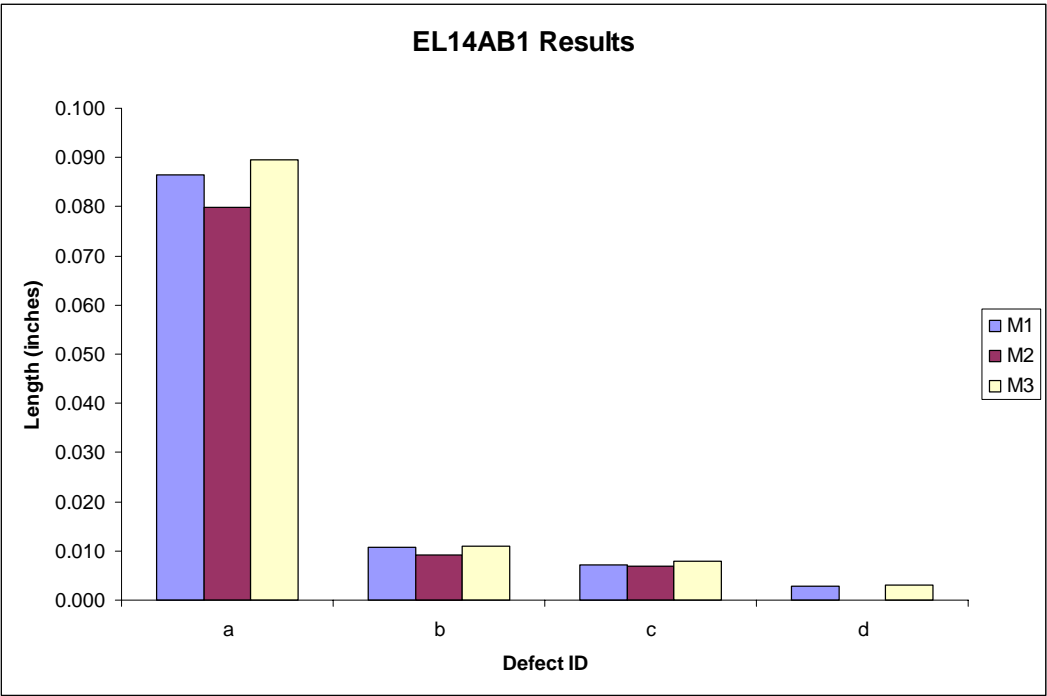


Figure 10. Measured defect indication lengths for fatigue cracks in the D6ac mousehole specimen EL14AB1 for field configurations M1, M2 and M3 (Appendix A). There is no significant difference in the length of the crack indications for the different field configurations.

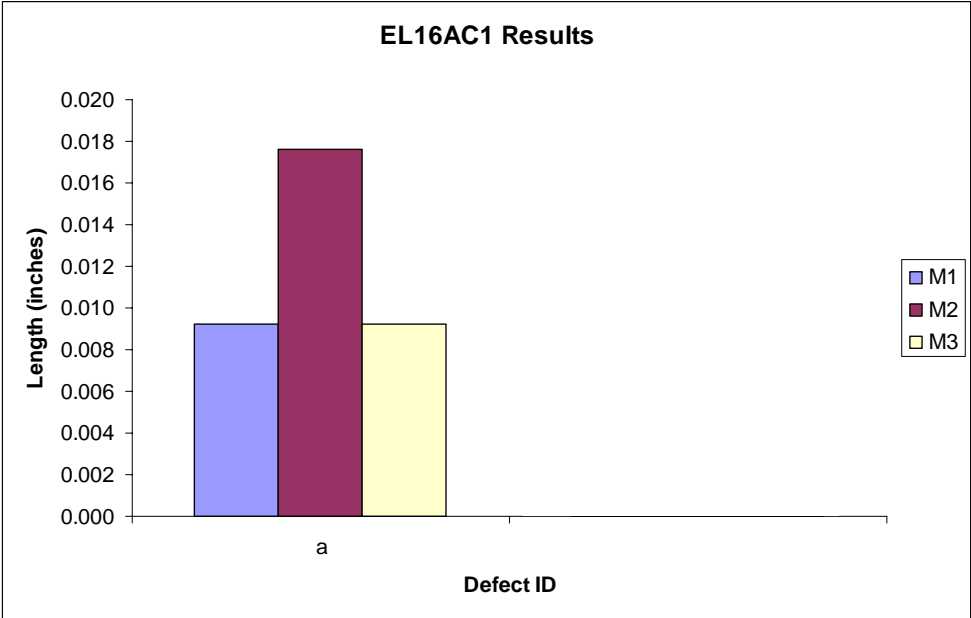


Figure 11. Measured defect indication length for the fatigue crack in the D6ac mousehole specimen EL16AC1 for field configurations M1, M2 and M3 (Appendix A). As discussed in section 2.3.3, there is no significant difference in the length of the crack indication due to the presence of the increased normal field component.

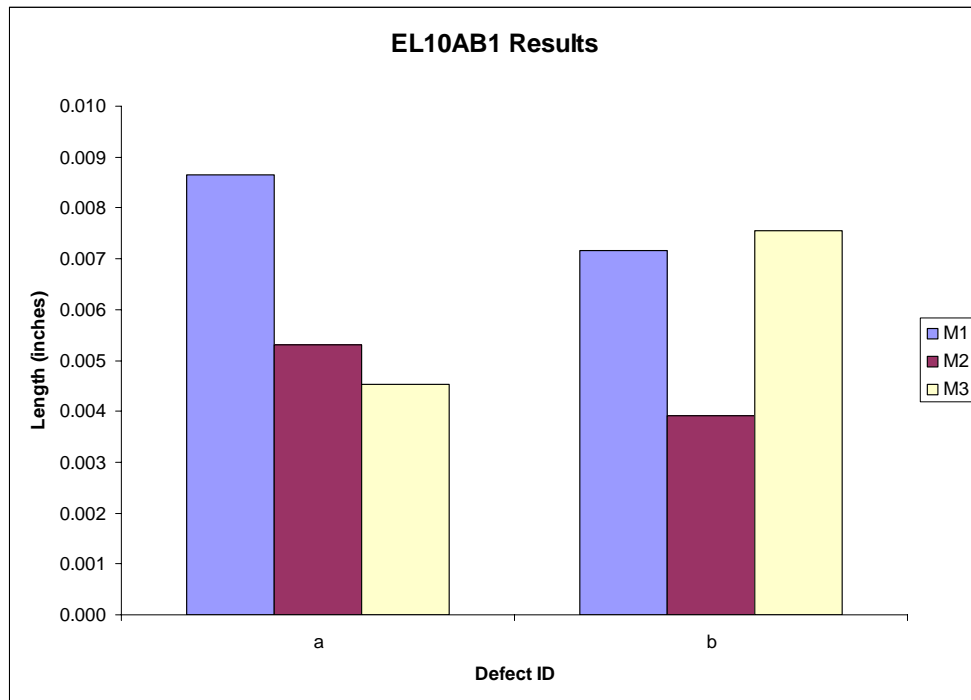


Figure 12. Measured defect indication lengths for fatigue cracks in the D6ac mousehole specimen EL10AB1 for field configurations M1, M2 and M3 (Appendix A). There is no significant difference in the length of the crack indications for the different field configurations.

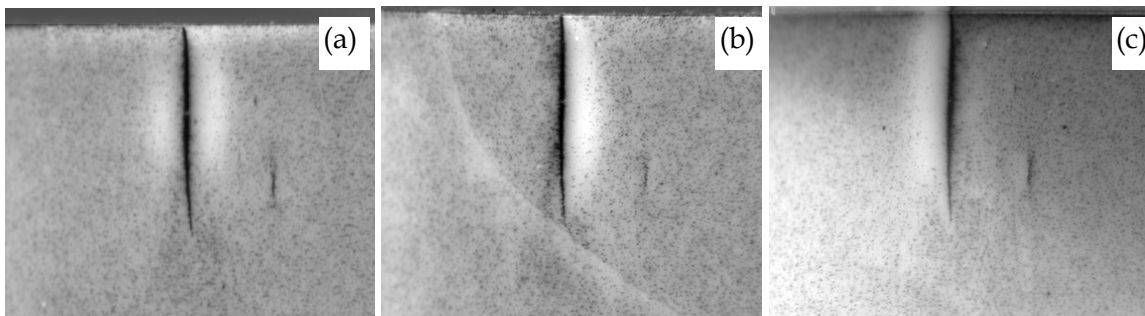


Figure 13. Photographs of MRT casts of cracks in the mousehole specimen EL14AB1. The tangential field in all cases is ~ 27 Gauss but the normal component of field varies from (a) 5 Gauss – a low value, (b) 27 Gauss – equivalent normal and tangential field amplitudes, and (c) -27 Gauss – normal field reversed in direction. Note that the location of the white band is reversed when the normal field is reversed. The larger crack is 0.090" long and the smaller crack is 0.012" long.

2.3.3 Mousehole Coupon Experiment: Analysis

The analysis sought to find any systematic reduction in the length of the crack indications due to the larger normal component of field.

The results given in Appendix A showed that the length of the indications differed by no more than $\sim 0.004''$ (corresponding to an individual error in length of $\sim \pm 0.002''$) when the normal field is increased from ~ 6 Gauss (M1) to 25 – 30 Gauss (M2 and M3) except for two of the defects, the large crack EL14AB1(a) and the defect EL16AC1(a). The result for EL16AC1(a) can be dismissed because the M2 indication is significantly longer than either the M1 or M3 indications and so it is likely to be a large systematic error or a mistake. For EL14AB1(a), the length of the M1 indication ($0.087''$) and the M3 indication ($0.089''$) are within the $\pm 0.002''$ tolerance but the M2 indication ($0.080''$) is not. This would only be significant if both the M2 and M3 indications were smaller than the M1 indication because the only difference between cases M2 and M3 is the sign of the normal field component. The difference is thus considered to be due to experimental error.

Hence, for the population of cracks examined in this trial, the presence of a normal field component with the same magnitude as the tangential field has no significant effect on the size of the MRT indications to within the expected experimental scatter. This conclusion is further supported by the results of a more sophisticated statistical analysis presented in Appendix C.

3. Discussion

As a result of these experiments, it can be recommended that when the normal field cannot be readily reduced to an insignificant level (< 6 Gauss), there is provision for the normal-to-tangential field ratio, B_n/B_t to be as great as 1, without significantly increasing the risk of a reduction in indication length or a significant reduction in intensity or clarity of crack indications.

A further potential inaccuracy introduced by the presence of a normal field, is that a slight deviation of a field-measurement device (Gaussmeter probe) from the tangential position, will result in a partial reading of the normal field. This could result in false or unreliable readings, particularly if the normal field is very large with respect to the tangential field B_t , and extra care should be taken. Thus, as the normal field increases, it becomes increasingly difficult to ensure that the tangential field is within the normally accepted range.

Despite an extensive search, no references to the role of normal fields in MRT (as such) could be located in the scientific literature. However, the significance of normal and tangential fields in magnetic particle inspection (MPI) is described in detail by Shelikov (2004), together with a detailed description of white banding and related phenomena. Shelikov recommends that the ratio of the normal to tangential field for MPI should be less than 3. This is less restrictive than the value of 1 proposed here for MRT. The underlying significance of Shelikov's work is that it was necessary to impose a restriction on the normal component of field for a closely-related magnetic inspection technique. Additional trials, along the lines of those described in

Section 2.3 but with a larger normal field component, would be required to establish if the normal field requirement could be further relaxed to a value approaching that suggested by Shelikov.

The detailed mechanisms leading to the reduced length of crack indications for large normal fields (observed in Sections 2.1 & 2.2) are not known. However, a relatively simple model for the forces on a magnetic particle in the vicinity of a crack can be modified to include a uniform normal field [Forster, 1982; McCoy and Tanner, 1990]. The result of a simple simulation of particle trajectories performed at DSTO is shown in Figure 14 for idealised particles on a regular grid with random velocities. The main effect of the normal field B_n in this simple geometry is to distort the leakage field so that the magnitude of the leakage field on one side of the crack exceeds that both immediately over the crack and on the other side of the crack. This results in the particles being preferentially drawn to one side of the crack, leaving a white band on the other side. These simulations also show the white band appearing on the opposite side of the crack when the normal field is reversed.

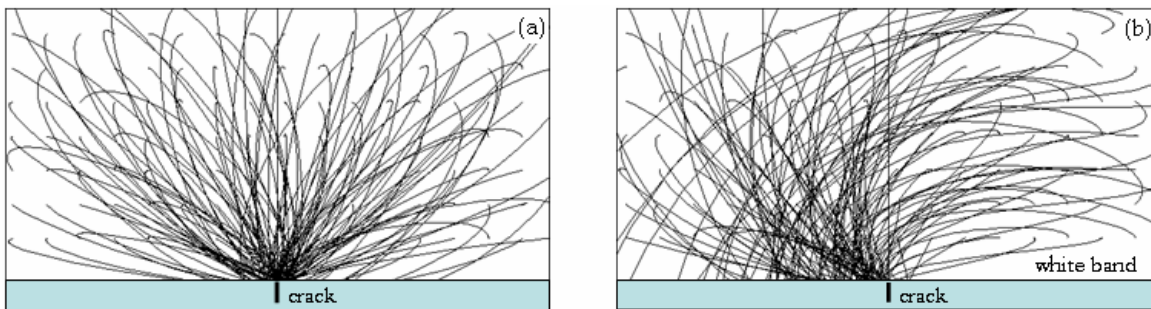


Figure 14. Simulation of the effect of the normal field on magnetic particles with random velocities. (a) Particles experiencing a tangent field only are drawn to the simulated crack. (b) Particles experiencing a tangent and normal field of comparable magnitude are forced to one side of the crack.

4. Conclusions

The experiments presented here confirm that excessive levels of normal (perpendicular) magnetic field in active-field MRT procedures can cause distortion, weakening or masking of indications from fatigue cracks. Consequently, when developing active-field MRT procedures, the levels of normal magnetic fields should be reduced as much as practicable. The experimental results show that, provided that throughout the test area the normal component of magnetic field does not exceed the tangential magnetic field, the presence of a normal magnetic field should not significantly reduce the sensitivity of active-field MRT.

The experimental results demonstrated that, for active-field MRT, a tangential field in the range 25 – 30 Gauss is suitable to provide clear MRT indications for the laboratory grown fatigue cracks in the test coupons.

Consequently, we conclude that an active-field MRT inspection developed to achieve 25 – 30 Gauss tangential magnetic field throughout the test area, and with the normal field not

exceeding the tangential magnetic field throughout the test area, should achieve the levels of sensitivity and reliability normally expected for active-field MRT.

The scope of this work did not include residual-field MRT and results should not be applied to any residual-field MRT procedures.

5. Recommendations

For active-field MRT, the normal component of magnetic field should not exceed the tangential component of magnetic field within the test area.

Further experiments should be performed, to confirm the relationship between the normal-to-tangential field ratio, and the clarity of indications in MRT casts. These experiments should include varying normal-to-tangential ratios, at different levels of tangential field.

6. Acknowledgements

The authors wish to acknowledge the invaluable contributions from DSTO and NDTSL staff, particularly, Mr Andy Deering (NDTSL), Dr Geoff Hugo and Cayt Harding (DSTO). We also wish to acknowledge the careful and expert work of the staff of AerostructuresNDT in performing the mousehole trials and in preparing the experimental results presented in Section 2.3 & Appendix A as well as for helpful discussions and constructive criticism.

7. References

- [1] F Forster (1982) "Nondestructive inspection by the method of magnetic leakage fields", *Defektoskopiya* **11** 3-25.
- [2] C A Harding and G R Hugo (2002) "Experimental Determination of the Probability of Detection for Magnetic Rubber Inspections of F-111 Steel Components", Defence Science and Technology Organisation, *DSTO-TN-0420*, Melbourne, Australia.
- [3] J M McCoy and B K Tanner (1990) "Computer Simulations of indications in magnetic particle inspection", *J.Phys.D: Appl.Phys.* **23** 593-599.
- [4] G S Shelikov (2004) "Dependence of the detectability of flaws on the distribution of the magnetising field in the vicinity of a flaw", *Russian J. NDT* **40** 52-65.
- [5] K C Watters (1997) "Strain Surveys of Fuel Flow Vent Hole Number 13 and Stiffener Runout Number 2 in the F-111 Wing Pivot Fitting for a Range of Rework Shapes", Defence Science and Technology Organisation, *DSTO-TR-0567*, Melbourne, Australia.

Appendix A: Normal-Tangent Field Trial Results

A summary of the results of the mousehole coupon trial performed by Aerostructures NDT (described in section 2.3) are presented here. The complete raw data sets and photos may be obtained from the authors on request.

| Specimen No. | Magnetic Field (G) | | | Crack identification and measured crack length on cast | | | | | | | | | | | | | |
|--------------|--------------------|---------|---------------|--|--------------|--------------|-------|--------------|--------------|--------------|--------------|-------|--------------|-------|--------------|-------|-------|
| | Normal | Tangent | Magnet Angle | a | b | c | d | e | f | g | h | i | j | k | l | m | n |
| EL3AC3 | 5.2 | 25.9 | M1 | 0.006 | 0.004 | 0.005 | 0.003 | 0.003 | 0.011 | 0.003 | 0.005 | 0.003 | | | | | |
| | 29.0 | 28.0 | M2 | 0.004 | 0.004 | 0.003 | 0.005 | 0.004 | 0.010 | 0.004 | 0.008 | 0.005 | | | | | |
| | 28.0 | 27.0 | M3 | 0.004 | 0.006 | 0.003 | 0.004 | 0.003 | 0.011 | 0.005 | 0.004 | 0.003 | | | | | |
| | | | <i>Master</i> | <i>0.006</i> | <i>0.005</i> | * | * | * | <i>0.012</i> | * | <i>0.005</i> | * | | | | | |
| EL3AF3 | 5.7 | 29.2 | M1 | 0.002 | 0.009 | 0.003 | 0.003 | 0.002 | 0.010 | 0.005 | 0.004 | 0.002 | 0.012 | 0.003 | 0.008 | 0.004 | 0.002 |
| | 27.4 | 27.1 | M2 | 0.002 | 0.008 | 0.005 | 0.003 | 0.000 | 0.006 | 0.006 | 0.004 | 0.003 | 0.014 | 0.004 | 0.008 | 0.004 | 0.002 |
| | 25.2 | 25.6 | M3 | 0.000 | 0.005 | 0.004 | 0.000 | 0.000 | 0.009 | 0.004 | 0.006 | 0.000 | 0.011 | 0.000 | 0.007 | 0.000 | 0.000 |
| | | | <i>Master</i> | * | <i>0.009</i> | * | * | * | <i>0.011</i> | <i>0.006</i> | <i>0.006</i> | * | <i>0.013</i> | * | <i>0.009</i> | * | * |
| EL8AK1 | 5.6 | 29.3 | M1 | 0.006 | 0.006 | 0.006 | 0.003 | 0.008 | 0.003 | 0.008 | 0.002 | 0.002 | 0.002 | | | | |
| | 30.1 | 30.0 | M2 | 0.006 | 0.005 | 0.005 | 0.004 | 0.007 | 0.007 | 0.007 | 0.003 | 0.002 | 0.002 | | | | |
| | 27.4 | 27.1 | M3 | 0.006 | 0.006 | 0.006 | 0.003 | 0.006 | 0.005 | 0.004 | 0.000 | 0.000 | 0.000 | | | | |
| | | | <i>Master</i> | <i>0.007</i> | * | <i>0.005</i> | * | <i>0.008</i> | * | * | * | * | * | | | | |
| EL14AB1 | 5.9 | 27.3 | M1 | 0.087 | 0.011 | 0.007 | 0.003 | | | | | | | | | | |
| | 26.8 | 27.4 | M2 | 0.080 | 0.009 | 0.007 | 0.000 | | | | | | | | | | |
| | 27.9 | 27.9 | M3 | 0.089 | 0.011 | 0.008 | 0.003 | | | | | | | | | | |
| | | | <i>Master</i> | <i>0.090†</i> | <i>0.012</i> | <i>0.008</i> | * | | | | | | | | | | |
| EL16AC1 | 5.6 | 25.2 | M1 | 0.009 | | | | | | | | | | | | | |
| | 26.8 | 26.2 | M2 | 0.018 | | | | | | | | | | | | | |
| | 29.8 | 30.1 | M3 | 0.009 | | | | | | | | | | | | | |
| | | | <i>Master</i> | <i>0.010†</i> | | | | | | | | | | | | | |
| EL10AB1 | 5.6 | 29.7 | M1 | 0.007 | 0.009 | | | | | | | | | | | | |
| | 30.1 | 30.0 | M2 | 0.005 | 0.004 | | | | | | | | | | | | |
| | 25.4 | 25.9 | M3 | 0.005 | 0.008 | | | | | | | | | | | | |
| | | | <i>Master</i> | <i>0.005</i> | <i>0.008</i> | | | | | | | | | | | | |

- Notes:
1. All crack lengths are measured in inches. Only bore cracks or the bore ligament of corner cracks (†) are tabulated
 2. *Master* data are the estimated true crack lengths from the earlier DSTO POD trial MRT master inspections performed under tensile load [Harding and Hugo 2002]. A star (*) for the master inspection value indicates that, while the small crack may have been detected, the crack length was not finally recorded in the POD study, as master crack lengths were recorded only for cracks $\geq 0.005"$ in size.
 3. Very small cracks (those with an average length less than 0.004") are displayed using a grey font
 4. A crack length of zero denotes that an indication seen for one of the other magnet angles is either absent or too small to be measured

Appendix B: Inspection Procedure

The following inspection procedure "MRT NORMAL/TANGENTIAL FIELD MEASUREMENTS" was used for the mousehole coupon experiments described in Section 2.3 and Appendix A.

MRT NORMAL/TANGENTIAL FIELD MEASUREMENTS

INTRODUCTION

1. **Operator Level.** III
2. **Method.** MRT
3. **Applicability.** Mousehole Test Specimens
4. **MRN.** Various
5. **Material.** D6ac Steel

NOTE

This Specific Procedure shall be used in conjunction with a General Procedure. Only information that emphasises, differs from, or is additional to the requirements of the General Procedure is included. All other procedural steps shall be performed in accordance with the General Procedure. The information laid down in this procedure takes precedence over the General Procedure.

6. **Reference Document.** This procedure is to be used in conjunction with AAP 7002.043-36 Sect 4 Chap 2 (MRT/GEN/1).

PURPOSE

7. The purpose of this test is to observe the properties of a Magnetic Rubber indication under varying conditions of normal and tangential magnetic field, applied to a corner crack in a mousehole specimen. Initially, three magnetisations and pours are to be performed on each specimen.

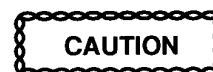
EQUIPMENT REQUIREMENTS

8. The following equipment is required:
 - a. Power shoe magnet including pole pieces and bridging (dampening) shims.
 - b. Gaussmeter with transverse probe.
 - c. Parker magnetising yoke.
 - d. Gauss measuring guide.
 - e. Additional equipment as detailed in MRT/GEN/1.

SAFETY PRECAUTIONS

9. As per MRT/GEN/1.

PRE-TEST REQUIREMENTS



D6AC STEEL COMPONENTS SHALL NOT BE LEFT IN AN UNINHIBITED CONDITION FOR OVER ONE HOUR. COAT UNINHIBITED COMPONENTS WITH THE APPROVED CORROSION INHIBITER, OR CORROSION WILL RESULT.

EQUIPMENT SETTINGS/SET-UP PROCEDURE

10. Carry out the set-up procedure in accordance with MRT/GEN/1 and the following:
 - a. Apply the Parker yoke to the face of the specimen containing the crack.
 - b. Select the AC setting on the yoke.
 - c. Energise the yoke, and remove from specimen while energised in order to demagnetise the specimen.
 - d. Using the Gaussmeter transverse probe, measure the field in the vicinity of the crack, and ensure it is less than 2 gauss. If not, repeat from 10a.
 - e. Repeat 10a-d for all measurements.

TEST PROCEDURE

11. Carry out the test in accordance with the MRT/GEN/1 and the following:
 - a. Insert the gauss measurement guide into the mousehole, taking care that the measurement location coincides with the crack location (ref. Figure P1).
 - b. Apply the magnet assembly to the specimen, in the required Position 1, 2 or 3 (ref. Figure P3-Figure P7).

NOTE

Install/remove gauss damping shims as required, to control the overall magnetic field strength.

- c. Insert the transverse Gaussmeter probe into the gauss measurement guide, and adjust magnet assembly to achieve the required tangential and normal field readings for each position (Figure P2).
- d. Record both the tangential and normal field values.
- e. Remove gauss measurement guide, taking care not to disturb magnet assembly.
- f. Prepare identification tag to be inserted into rubber before it cures. Tag should be labelled with: Specimen number, magnet position (M1, M2 or M3), pour number and date. e.g. "EL3AC1 M1 #2 2/10/05"
- g. Build dam around mousehole, and pour pre-determined magnetic rubber mixture.
- h. Gently insert identification tag into top of rubber before it cures.
- i. Remove the cured cast and place it into a re-sealable plastic bag, suitably identified with the specimen number, magnet assembly position, levels of normal and tangential field, and date of test.
- j. Examine each cast under low magnification and photograph relevant indications at consistent levels of magnification. Include scaling bars.
- k. Demagnetise specimen IAW paragraph 10.
- l. Repeat a-k for all measurements.

MEASUREMENT POSITIONS

- 12. Casts will be poured and measurements performed in three different orientations of the magnet assembly:
 - a. Position 1 (ref. Figure P3-Figure P5). The measured tangential field should be 25 – 30 gauss, and the measured normal field should be less than 5 gauss.
 - b. Position 2 (ref. Figure P6). Rotate the magnet assembly to achieve a tangential-to-normal field ratio of 1:1. The target gauss level for each direction is 25 – 30 gauss.

- c. Position 3 (ref. Figure P7). Rotate the magnet assembly in the opposite direction to (b) to achieve a tangential-to-normal field ratio of -1:1. The target gauss level for each direction is \pm (25 to 30) gauss.

POST-TEST REQUIREMENTS

- 13. Demagnetise specimen using magnetising yoke as per § 10. Apply corrosion inhibitor to mousehole region of specimen.

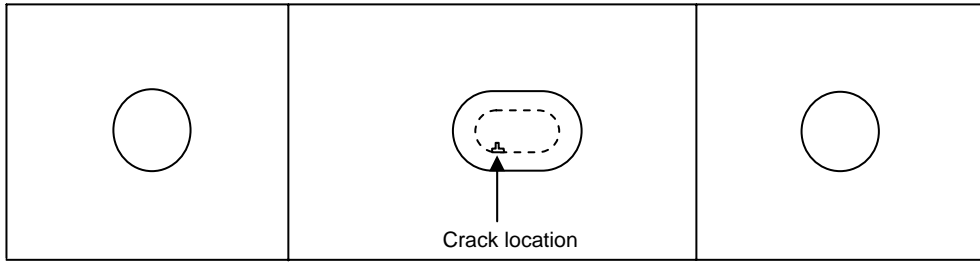


Figure P1. Mousehole specimen, gauss measurement guide inserted in mousehole.

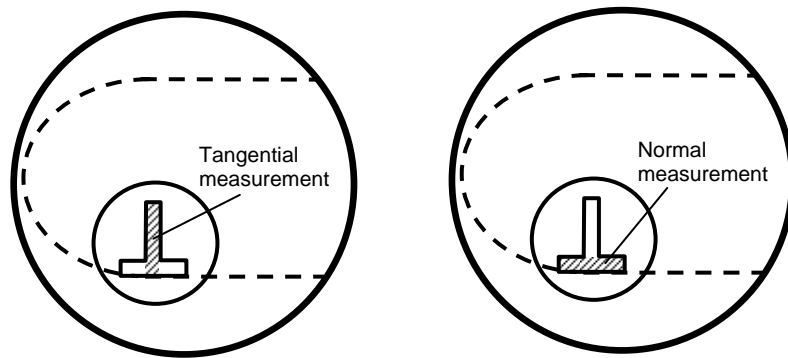


Figure P2. Detail of gauss measurement guide, showing probe orientation (thatched).

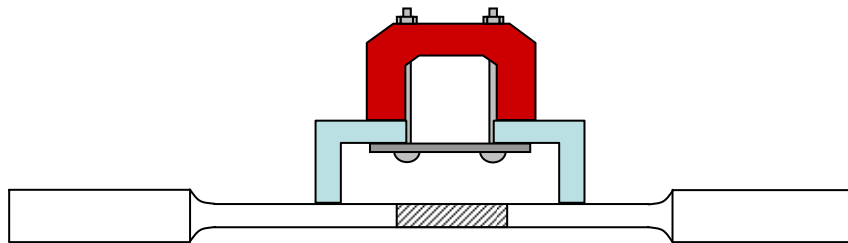


Figure P3. Magnet assembly applied to specimen in position 1. The assembly is progressively rotated to achieve the required normal and tangential field levels.

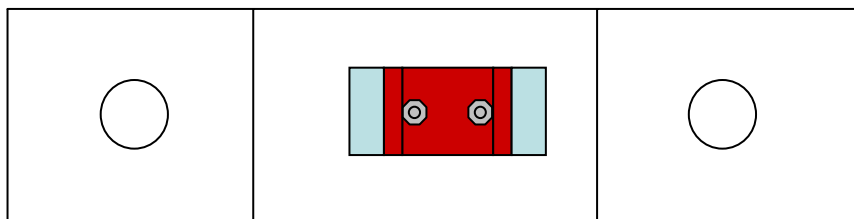


Figure P4. Plan view of magnet assembly applied to specimen in position 1.

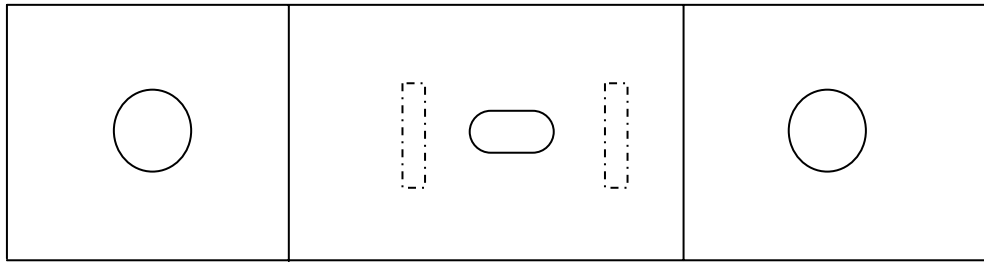


Figure P5. Position 1. Feet of pole pieces shown (dashed line) in relation to mousehole. Tangential field level is 25-30 gauss, and normal field level is maximum 5 gauss.

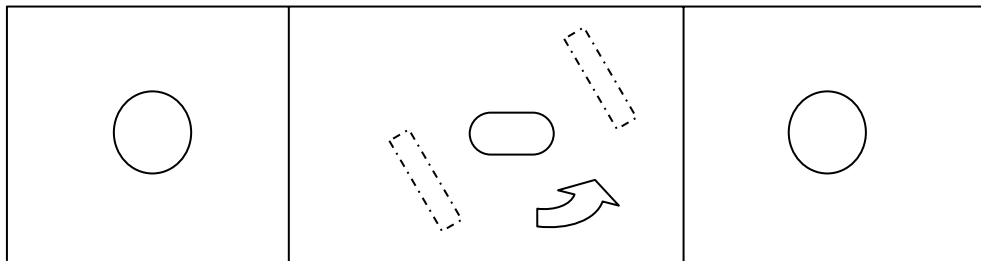


Figure P6. Position 2. The magnet assembly is rotated about the centre of the mousehole, to achieve a normal-to-tangential field ratio of 1:1. Target field level is 25 – 30 gauss.

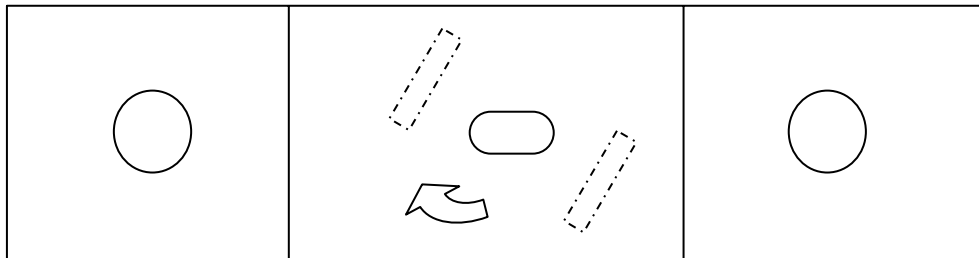


Figure P7. Position 3. Rotate magnet assembly in opposite direction to Position 2, to achieve a normal-to-tangential field ratio of -1:1. Target field level is \pm (25 to 30) gauss.

Appendix C: Statistical Analysis of the Lengths of MRT Indications for the Cases M1, M2 and M3

C 1 Experimental Scatter

In Section 2.3.3, it was stated that the individual error (or scatter) in the measured length of the indications was $\sim \pm 0.002''$. This value is consistent with the work of Harding and Hugo (2002) in which the lengths of a series of 35 MRT crack indications obtained under tensile load were compared with fractography for the same cracks. For cracks in the range $0.003''$ to $0.030''$, the standard deviation in the difference between the fractographic data and the MRT indication lengths was $0.0016''$. Taking the scatter in the fractography to be zero, the scatter in the length of MRT indications is therefore $\pm 0.0016''$ or, rounding up, $\sim \pm 0.002''$. This value is consistent with the observed scatter in the difference in the lengths of the indications M2 and M3 in Appendix A.

Note that the scatter of $\pm 0.002''$ in the measured length of the indications is not related at all to the accuracy of a_{NDI} derived from the MRT POD trials. In the POD trials, hit/miss data were collected for cracks of known size⁶ and the accuracy of the NDT technician's measurement of the length of indications was not relevant.

C 2 Tests of Statistical Significance

The statistical significance of the results presented in Section 2.3 and Appendix A was examined further using a "paired two sample t-Test". The analysis was performed using *Origin* (Version 7.0) statistical hypothesis testing routines and was restricted to cracks longer than $0.003''$ to avoid unwanted bias from very small cracks.

The principal results are summarised below.

Are the M1 indications shorter than the master crack length?

Data set: All master data and associated M1 indication lengths in Appendix A (19 pairs).

Observation: For this data set, the M1 indications were on average 0.6 thousandths of an inch shorter than the corresponding master lengths. The statistical significance of this difference was assessed using a paired t-test.

Null hypothesis H_0 : $\mu_{\text{M1}} \geq \mu_{\text{MASTER}}$

Alternate hypothesis H_A : $\mu_{\text{M1}} < \mu_{\text{MASTER}}$

⁶ The crack lengths were known from fractography and other analyses.

Paired t-test: The t-statistic $t = 2.43$ is significant at the 0.05 level (P value = 0.013), therefore the null hypothesis is rejected. The mean M1 length is smaller than the mean master length at a 0.05 level of statistical significance.

Conclusion: These results indicate that the M1 indications are on average slightly shorter than the corresponding master lengths. This is to be expected because the master crack data were obtained with the specimen under a tensile load whereas the M1 data were obtained with no applied load.

Are the M2 and M3 indications the same length?

Data set: All M2 and M3 data in Appendix A for which the average length⁷ of the indications is greater than or equal to 0.003" excluding the 0.090" crack EL14Ab1a and crack EL16AC1 as discussed in Section 2.3.3. (27 pairs)

Observation: For this data set, the M2 indications were on average 0.4 thousandths of an inch shorter than the corresponding M3 indications. The statistical significance of this difference was assessed using a paired t-test.

Null hypothesis H_0 : $\mu_{M2} = \mu_{M3}$

Alternate hypothesis H_A : $\mu_{M2} \neq \mu_{M3}$

Paired t-test: The t-statistic $t = 1.049$ is not significant at the 0.05 level (P value = 0.303) so there is not enough evidence to reject the null hypothesis at this level of statistical significance.

Conclusion: The results indicate that the mean lengths of the M2 and M3 indications are not different at a 0.05 significance level. This is expected because reversing the normal field would not have any obvious physical effect on the length of the indication to first order.

Are the M2 indications shorter than the M1 indications?

Data set: All M1 and M2 data in Appendix A for which the average length of the indications is greater than or equal to 0.003" excluding the 0.090" crack EL14Ab1a and crack EL16AC1 as discussed in Section 2.3.3. (27 pairs)

Observation: For this data set, the M2 indications were on average 0.05 thousandths of an inch shorter than the corresponding M1 indications. The statistical significance of this difference was assessed using a paired t-test.

Null hypothesis H_0 : $\mu_{M2} \geq \mu_{M1}$

Alternate hypothesis H_A : $\mu_{M2} < \mu_{M1}$

⁷ For these sorting purposes the average length of the indication was taken to be $(M1+M2+M3)/3$.

Paired t-test: The t-statistic $t = 0.123$ is not significant at the 0.05 level (P value = 0.451) so the null hypothesis cannot be rejected.

Conclusion: On the basis of these results, there is insufficient statistical evidence to prove that the M2 indications are shorter than the M1 indications. Any reduction in the length of the indications (if it exists) is small and lies well within the experimental scatter.

Are the M3 indications shorter than the M1 indications?

Data set: All M1 and M3 data in Appendix A for which the average length of the indications is greater than or equal to 0.003" excluding the 0.090" crack EL14Ab1a (28 pairs)

Observation: For this data set, the M3 indications were on average 0.4 thousandths of an inch shorter than the corresponding M1 indications. The statistical significance of this difference was assessed using a paired t-test.

Null hypothesis H_0 : $\mu_{M3} \geq \mu_{M1}$

Alternate hypothesis H_A : $\mu_{M3} < \mu_{M1}$

Paired t-test: The t-statistic $t = 0.489$ is not significant at the 0.05 level (P value = 0.074) so the null hypothesis cannot be rejected.

Conclusion: On the basis of these results, there is some evidence that the M3 indications are shorter than the M1 indications but it is not statistically significant at the 0.05 level. Any reduction in the length of the indications (if it exists) is so small (< 0.5 thousandths of an inch) that it would have an insignificant effect on the POD for Magnetic Rubber Testing.

